ISSN: 0975-8585

Research Journal of Pharmaceutical, Biological and Chemical Sciences

Antimicrobial Activity and *In-Silico* Analysis of 3, 5, 6-Trichloro-2-Pyridinol.

Dhaya Rani Varkey, Danie Kingsley J, and Jayanthi Abraham*.

Microbial Biotechnology Laboratory, School of Biosciences and Technology, VIT University, Vellore 632014, Tamil Nadu, India.

ABSTRACT

Penicillin binding proteins have been a well established target for antimicrobial therapy. β-lactum antibiotics the widely used inhibitor for PBPs inhibits the transpeptidase activity of PBPs by forming a covalent penicilloyl-enzyme complex which blocks the normal transpeptidation reaction; resulting in bacterial death. Resistant bacteria tend to distort the active site of PBP thereby lowering their acylation efficiency for β-lactams. We have tried to find a solution for this problem with the use of noncovalent inhibitors of PBPs. In order to explore the possibilities of a new drug, 3, 5, 6-trichloro-2-pyridinol (TCP) the hydrolysis product of Chlorpyrifos a broad spectrum moderately toxic organophosphorus insecticide was chosen in this present study. This is the first study which focuses on the use of TCP as a likely drug candidate against commonly encountered pathogens. Four Gram negative bacterial pathogens *Escherichia coli* (3MZD and 1NZO), *Pseudomonas aeruginosa, Shigella dysenteriae* and *Klebsiella pneumoniae* and two Gram positive bacterial pathogens *Staphylococcus aureus* and *Streptococcus pneumoniae* were selected for this study and were identified using standard biochemical tests. TCP had a good inhibitory effect against these pathogens, it was found to be most effective against *Pseudomonas aeruginosa* and *Staphylococcus aureus* with a zone of inhibition of 22mm and 21mm respectively. TCP was equally effective against *Salmonella typhimurium, Shigella dysenteriae, Klebsiella pneumoniae* and *Escherichia coli* -3MZD (20mm each). Insilico analysis was also performed by choosing Penicillin Binding Proteins of the microbes as the target protein sequence. iGEMDOCK is the docking tool used for docking TCP against all of these PBPs. *Pseudomonas aeruginosa* registered the best docking score of -66.5(which correlates with 22mm zone of inhibition) followed by the others.

Keywords: Chlorpyrifos, 3, 5, 6-trichloro-2-pyridinol, *Penicillin* Binding Proteins, iGemdock.

Corresponding author

ISSN: 0975-8585

INTRODUCTION

For the past several decades the incidence of bacteria becoming resistant to well known antibiotics is in the rise. In contrast over the past 30 years the development of novel antimicrobial agents against resistant strains has been declining [1]. The root causes for hospital acquired bacterial resistance has been attributed to factors such as antimicrobial effects in treated individuals, mechanisms for transfer of resistance between bacteria and routes of transmission within the hospital [2].The intense use and misuse of antibiotics were undoubtedly the major causes associated with the high numbers of resistant pathogenic and commercial bacteria worldwide [3]. Hospital consumption of tetracycline, first and second generation cephalosporins, third-generation cephalosporins and quinolones has led to quinolone-resistant *E. coli* isolates [4]. Drug resistant organisms mostly lead to ultimate death of the patient after prolonged illness [5]. It has also been proven that plasmids and bacterial strains are found to be mediating multi-drug resistance in hospital acquired infections, which have their origin in the same hospital premises [6].

There has been a gradual increase in drug resistant pathogens, including methicillin-resistant *Staphylococcus aureus* (MRSA), vancomycin-resistant *Enterococcus* (VRE) [7] multidrug-resistant (MDR) *Pseudomonas aeruginosa*, imipenem-resistant *Acinetobacter baumannii* [8] third-generation cephalosporin-resistant *Escherichia coli* [9] and *Klebsiella pneumoniae* which pose a serious threat. Data from the Study for Monitoring Antimicrobial Resistance Trends (SMART) has revealed that Asia-Pacific countries have the highest level of antimicrobial resistance [10].

Investigation of herbal extracts of *Aloe-vera*, Neem, Guava (*Psidium guajava*), Pomegranate (*Punica granatum*) and tea (*Camellia sinensis*) can be used as therapeutics against MRSA infections [13]. The antimicrobial activity of different phenolic compounds identified and quantified in mushroom species from all over the world was evaluated; its structure–activity relationship (SAR) analysis and molecular docking studies were performed and it was concluded that 2,4-Dihydroxybenzoic and protocatechuic acids were the phenolic compounds with higher activity against the majority of Gram negative and Gram positive bacteria[14].

3, 5, 6-trichloro-2-pyridinol is a metabolite of Chlorpyrifos which is an organophosphorus pesticide. 3, 5, 6-trichloro-2-pyridinol and 2-methoxy 3, 5, 6-trichloropyridine does have antimicrobial activity against *Sclerotium solfsii* a facultative plant pathogen [11]. It is also reported that TCP and its derivatives also possess anti-microbial effects against Gram negative bacteria *Escherichia coli* and Gram positive bacteria *S. albicans* [12]. However, not much work is carried on regarding the antimicrobial activity of 3, 5, 6-trichloro-2-pyridinol (TCP). Hence, this research work was focused on screening for antimicrobial activity of 3, 5, 6-trichloro-2-pyridinol on various clinical pathogens and ascertain it with computational analysis.

MATERIALS AND METHODS

Microbial Cultures

The pathogenic bacterial cultures used in this present study were procured from Microbial Biotechnology Lab, SBST, VIT University, Vellore, Tamilnadu. All of the isolates were subjected to morphological and biochemical tests (Table 1) and the test results were compared with Bergey's manual.

Table 1: Biochemical profile of clinical pathogens

Biochemical test / Isolates	Gram's Staining	Catalase	Glucose Oxidase	Indole	Citrate	MR	VP	Urea	Gas from Glucose	Mannitol
E.coli (3MZD)	-, Rod	+	+	+	-	+	-	-	+	+
E.coli (1NZO)	-, Rod	+	+	+	-	+	-	-	+	+
Pseudomonas aeruginosa	-,	+	-	-	+	-	-		-	-
Salmonella typhimurium	-, Rod	+	-	-	-	+	-	-	-	
Staphylococcus aureus	+, Cocci	+	+	-	-		+	+		+
Shigella dysenteriae	-, Rod	-	-	+	-	+	-	-	-	+
Streptococcus pneumoniae	+, Cocci	-	-			+	-	-		+
Klebsiella pneumoniae	-, Rod	+	-	-	+	-	+		+	+

Chemical and Reagents

The chemicals and reagents used were of analytical grade, TCP (3, 5, 6-trichloro-2 pyridinol) was purchased from Sigma laboratories. The collected specimens were sub cultured and stored for further analysis.

Experimental

Antibacterial Activity assessment of TCP

Antibacterial activity was evaluated by well diffusion method on nutrient medium. This was confirmed by the inhibitory effect on bacterial growth reflected by the zone of inhibition. The sterile nutrient agar medium in petri dishes was innoculated with the isolated clinical pathogenic bacteria cultures viz, *Escherichia coli* (3MZD and 1NZO)*, Pseudomonas aeruginosa, Salmonella typhimurium, Shigella dysenteriae* and *Klebsiella pneumoniae, Staphylococcus aureus* and *Streptococcus pneumonia.* Wells of 5mm were made in the petri plates. Four different concentrations of TCP (50 µg, 100 µg, 150 µg and 200 µg) were evaluated. For each treatment triplicates were maintained. The plates were incubated at 37°C for 24 h and the resulting zone of inhibition was measured.

Data sets for *in silico* study

The crystal structure of penicillin binding proteins for the various microbe's viz., *Escherichia coli* (3MZD and 1NZO), *Pseudomonas aeruginosa,* and *Staphylococcus aureus* were selected for this study. The PBP structures were obtained from the Research Collaboratory for Structural Bioinformatics (RCSB) protein databank (PDB) [15].

The PDB id *Escherichia coli*_1s 3MZD was selected for structural analysis based on its high resolution crystallographic structure (1.90Å resolution). Similarly, the PDB id for the PBP of *Escherichia coli*_2, *Pseudomonas aeruginosa,* and *Staphylococcus aureus* are 1NZO, 3OC2, and 1TVF respectively was selected. These PBPs were selected based on its high resolution crystallographic structure of 1.85Å resolution, 1.97Å resolution, and 2.00 Å resolutions respectively. The crystallographic water molecules and co-crystalised ligands were identified and removed from the 3-dimensional (3D) atomic coordinate file. The structure of 3, 5, 6-trichloro-2-pyridinol (TCP)-PBD CID (23017) were sketched using CHEMSKETCH software (ACD/ChemSketch, version 11.0). The 3-Dimensional molecular models for the ligands were generated with the help of 3D structure conversion server Corina. Energy minimization of ligands was done by using chimera software [16].

Homology Modeling and structure validation

In the lack of an experimentally established crystal structure of Penicillin Binding protein, homology modeling is the best alternative to construct a reasonable three- dimensional (3D) model of the target. At present, computational modeling is the most accurate technique for 3D structure prediction of proteins. The protein sequence of *Shigella dysenteriae*, *Klebsiella pneumoniae. Salmonella typhimurium* and *Streptococcus pneumoniae* in FASTA format was obtained from the UNIPROT database [17]. Further, these FASTA sequences were used to construct the 3D PBP Co-ordinates with the help of I-TASSER server. I-TASSER server is an on-line platform for protein structure and function predictions. 3D models are built based on multiple-threading alignments by LOMETS and iterative template fragment assembly simulations; function insights are derived by matching the 3D models with BioLiP - PROTEIN FUNCTION DATABASE.

Among the generated 3D structures the structure with the least C- score was selected for further analysis. C-score is a confidence score for estimating the quality of predicted models by I-TASSER. It is calculated based on the significance of threading template alignments and the convergence parameters of the structure assembly simulations. C-score is typically in the range of [-5, 2], where a C-score of higher value signifies a model with a high confidence and vice-versa.

PROCHECK [18] server was used for model quality evaluation. PROCHECK analysis includes checks on chirality, dihedral angles, planarity, disulphide bonds, covalent geometry non-bonded interactions, stereo chemical parameters, main-chain hydrogen bonds, parameter comparisons, and residue-by-residue analysis. Ramachandran plot was used for predicting the backbone conformation of Phi and Psi angles. The

Ramachandran plot for *Shigella dysenteriae* (Fig 1), *Streptococcus pneumoniae* (Fig 2), *Klebsiella pneumoniae* (Fig 3) and *Salmonella typhimurium* (Fig 4) are provided.

Active Site Prediction

Insilico prediction of binding sites of the various Penicillin Binding Proteins and was achieved using Qsite finder, [19] an energy-based method for the prediction of protein–ligand binding sites.

Docking

Docking was performed by iGEMDOCKv2.1 [20] this docking tool works effectively based on the genetic algorithm (GA) using virtual screening as the default tool. The automated molecular docking simulations were performed by Genetic Algorithm- Local Search (GA-LS) [21] with standard parameters. The compounds were ranked based on the docking energy. The compound with the highest affinity for the target proteins active site pattern with lowest docking energy was selected. Vander Waals energy, electrostatic energy and intermolecular hydrogen bonding and inhibition were calculated for each docked complex (Table 5). PyMol software (PyMOL Molecular Graphics System) was used for visualizing and analyzing the various docked structures.

Drug Scan

The drug likeness and other molecular properties and bioactivity score for TCP was carried out with the help of Molinspiration server [22]. The smiles format of the ligand TCP was provided as the input to obtain the above mentioned properties.

This was carried out in order to ascertain that the ligand of interest obeys Lipinski's Rule 5 to be a likely drug candidate [23]. The rule describes that the molecular properties are crucial for a drug's pharmacokinetics in the human body, including their absorption, distribution, metabolism and excretion of these compounds are checked for the drug-likeliness and the results are shown in Table 3.

Table 3: Molecular properties and drug likeness of the Ligand

S.No	Compound	PubChem CID	Molecular Weight[g/mol]	LogP (Octanol-water partition coefficient value)	H-Bond Donor	H-Bond Acceptor
1.	3 5 6-trichloro-2-pyridinol	23017	198.4336	2.617	2	1

RESULTS AND DISCUSSION

TCP (3,5,6-trichloro-2-pyridinol) the ligand under study, qualifies to become a good drug candidate since its molecular weight is less than 500, H-bond donors are less than 5, H bond acceptors are less than 10 amd Log P value is less than 5 which fulfills all of the requirements for a drug candidate. This would be an effective drug molecule.

Table 2: Antimicrobial activity of TCP against various clinical pathogens (Zone of inhibition)

S.no	TCP / Strain ID	50µg	100µg	150µg	200µg
1.	*E.coli* (3MZD)	10mm	15 mm	14 mm	20 mm
2.	*E.coli* (1NZO)	9 mm	11 mm	14 mm	17 mm
3.	*Pseudomonas aeruginosa*	12 mm	12 mm	16 mm	22 mm
4.	*Salmonella typhimurium*	8 mm	12 mm	14 mm	20 mm
5.	*Staphylococcus aureus*	7 mm	9 mm	12 mm	21 mm
6.	*Shigella dysenteriae*	11 mm	22 mm	15 cm	20 mm
7.	*Streptococcus pneumoniae*	8 mm	10 mm	11 mm	18 mm
8.	*Klebsiella pneumoniae*	10 mm	15 mm	14 mm	20 mm

ISSN: 0975-8585

The identified Gram negative bacteria were *Escherichia coli* (3MZD and 1NZO), *Pseudomonas aeruginosa, Salmonella typhimurium, Shigella dysenteriae* and *Klebsiella pneumonia* and Gram positive bacteria were *Staphylococcus aureus* and *Streptococcus pneumoniae*. The Biochemical test results are given in Table 1. The effect of TCP against the pathogenic bacteria cultures is presented in Table 2. TCP was found to be very effective against *Pseudomonas aeruginosa* with a zone of inhibition of 22mm, which was followed by *Staphylococcus aureus* (21mm) and *Escherichia coli* (3MZD), *Salmonella typhimurium, Klebsiella pneumoniae* and *Shigella dysenteriae* (each 20mm).

The 3D structural model of Penicillin Binding Proteins generated by homology based model has been examined by their stereo-chemical quality, by Procheck.

The Ramachandran plot for *Shigella dysenteriae* showed that phi/psi angles distribution of 90.1% residues were in the most favored regions, 7% residues were found in the additional allowed regions and 0.9% fell in the generously allowed regions; only 2% of residues were in the disallowed conformations (Fig.1). This analysis confirmed that the quality of the modeled PBPs was almost in good grade.

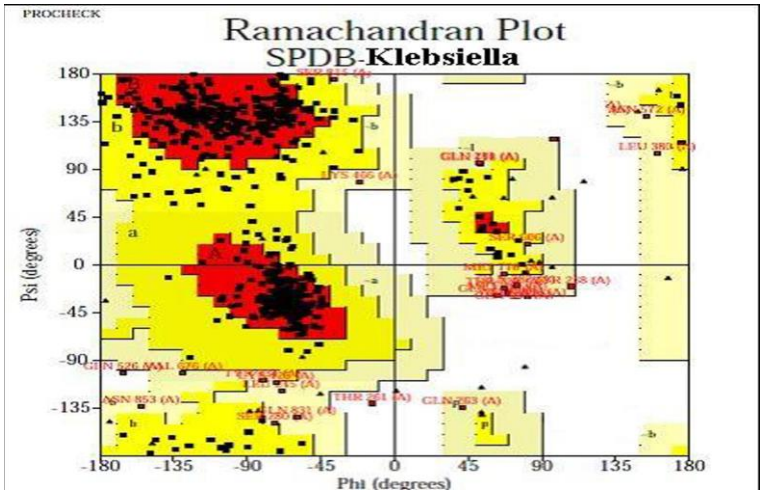

Figure 1: Ramachandran plot of the ϕ–ψ distribution of *Shigella dysenteriae* produced by PROCHECK [A, B, L] most favored regions; [a, b, l, p] additional allowed regions; [~a, ~b, ~l, ~p] generously allowed regions; white areas are disallowed regions. The plot shows 90.1% of amino acid residues of final model structure present in the most favoured region, 7% in additional allowed region, indicating the high quality of the model.

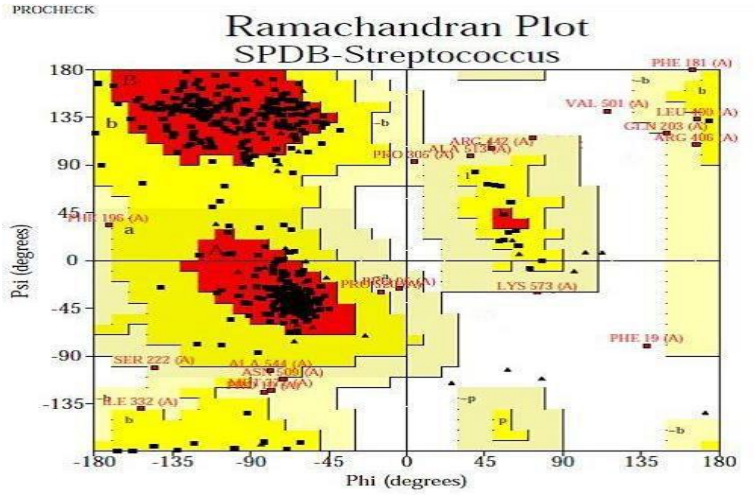

Figure 2: Ramachandran plot of the ϕ–ψ distribution of *Streptococcus pneumoniae* produced by PROCHECK [A, B, L] most favored regions; [a, b, l, p] additional allowed regions; [~a, ~b, ~l, ~p] generously allowed regions; white areas are disallowed regions. The plot shows 91.1% of amino acid residues of final model structure present in the most favoured region, 8.0% in additional allowed region, indicating the high quality of the model.

ISSN: 0975-8585

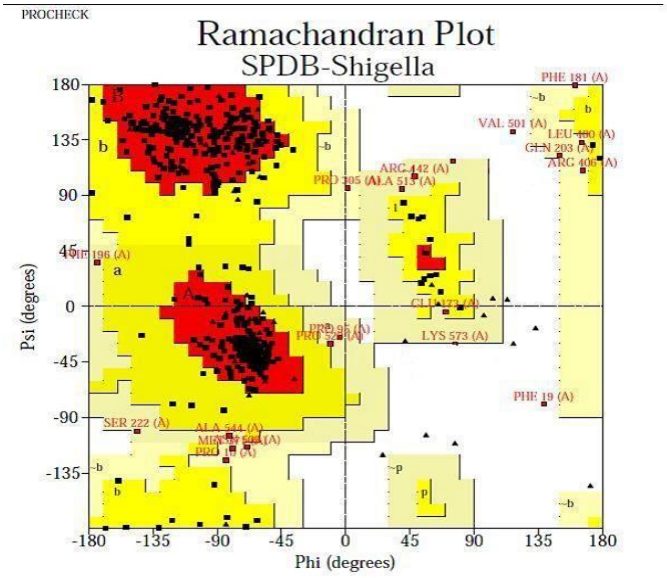

Figure 3: Ramachandran plot of the ϕ–ψ distribution of *Klebsiella pneumoniae* produced by PROCHECK [A, B, L] most favored regions; [a, b, l, p] additional allowed regions; [~a, ~b, ~l, ~p] generously allowed regions; white areas are disallowed regions. The plot shows 90% of amino acid residues of final model structure present in the most favoured region, 8.0% in additional allowed region, indicating the high quality of the model.

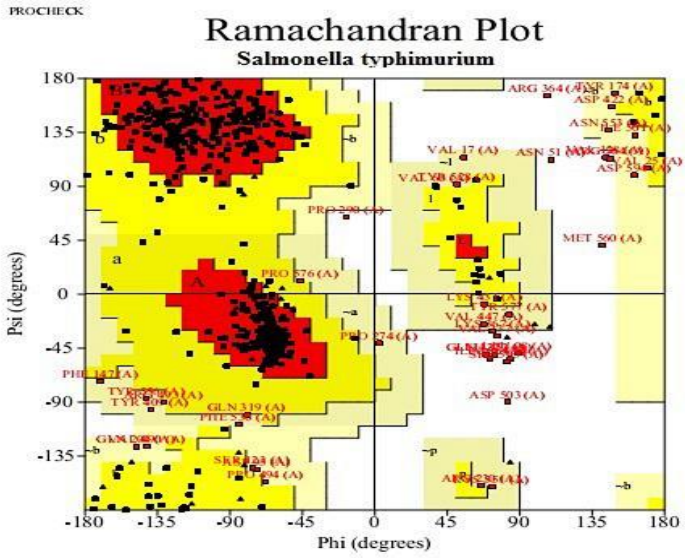

Figure 4: Ramachandran plot of the ϕ–ψ distribution of *Salmonella typhimurium* produced by PROCHECK [A, B, L] most favored regions; [a, b, l, p] additional allowed regions; [~a, ~b, ~l, ~p] generously allowed regions; white areas are disallowed regions. The plot shows 79.6% of amino acid residues of final model structure present in the most favoured region, 13.4% in additional allowed region, indicating the high quality of the model.

Similarly the Ramachandran plot for *Streptococcus pneumoniae* showed phi/psi angles distribution with 91.1% residues in the most favoured region, 6% residues lie in the additionally allowed regions and 1% in the generously allowed regions; while only 1.9% of residues were in the disallowed conformations (Fig. 2).

Likewise the Ramachandran plot for *Klebsiella pneumoniae,* shows that phi/psi angles distribution with 90% residues in the most favoured region, 8% residues lie in the additionally allowed regions and 1.5% in the generously allowed regions; while only 0.5% of residues were in the disallowed conformations (Fig. 3).

ISSN: 0975-8585

The Ramachandran plot for *Salmonella typhimurium*, shows phi/psi angles distribution with 79.6% residues in the most favoured region, 13.4% in the additionally allowed regions while only 4.5% and 2.6% are present in generously allowed and disallowed regions (Fig. 4)

Among the ten sites obtained from Q-site Finder, site 2 is found highly conserved in PBPs, therefore site 2 is chosen as binding site for docking study. The active site amino acids strings are mentioned in Table 4.

Table 4: Active site details of the PBPs

PBPs	PDB ID	Name of the organism	Active site residues
1	3MZD	*E.coli* (3MZD)	ILE5,LYS6, THR7,MET8,PRO10,ARG261,PHE262,PRO301, ARG302, ARG304.
2	1NZO	*E.coli* (1NZO)	ASN26, GLU230, GLY231, GLN232, MET233, ARG234, PHE260, GLU264, THR265, VAL266, ASN267
	3OC2	*Pseudomonas aeruginosa*	ALA162, HIS163, GLY166, PHE167, ARG175, GLU176, GLY177, LEU180.
4	1TVF	*Staphylococcus aureus*	ASN72, ALA74, SER75, LYS78, GLU114, LEU115, SER116, ASN141, THR180, GLY181, ALA 182, GLU183, ARG186, SER 262, SER 262, ASP 264, THR 265, TYR 291
5	Model 1	*Shigella dysenteriae*	HIS16, ALA17, ASN18, SER21, TRP22, SER381,ARG382, PHE383, GLY384,LYS387,THR389, ARG430,TYR441, ARG442, PRO443, VAL453, PRO454, GLY455, GLU456.
6	Model 2	*Streptococcus pneumoniae*	ASP92,ARG94,PHE95,ASP97,HIS98,ARG99,GLY100, ILE101, ASP102, ARG105, PHE110, SER118, LEU119, SER123, ALA124, THR126, GLN127, ALA151, ALA154, ILE155, GLU158
7	Model 3	*Klebsiella pneumoniae*	LEU 224, ASP22, THR228, ALA231, THR232, LEY344, ASP345, VAL376, LEU377, ARG378, LEU379, LEU380, GLN381, GLN382, GLN383, GLN384, VAL385, ILE386 ,GLU389
8	Model 4	*Salmonella typhimurium*	TRP 366, LYS 367, LYS 368, GLU 382, SER 383, ALA 384, ALA 522, PRO 523, SER 542, GLY 543, THR 544, TYR 571, ASP 594, GLY 595, VAL 596

The docking analysis was done for the Ligand TCP (3, 5, 6-Trichloro-2-pyridinol) with the target Penicillin Binding proteins of above mentioned bacteria by using the docking software GemDock. All compounds were docked into the binding site, and the docking data were analyzed using the lowest-energy docking modes. The docking scores of most potent ligands of different datasets are listed in Table 5. The binding affinity of the ligands with target proteins has been analyzed from the binding energy, inhibition constant and H-bonds.

Table 5: Docking Results of TCP with the PBP of Targets

S.No	PDB ID	Organism	Protein Type	Energy	VDW	Z Score	Interaction Profile
1.	3MZD	*E.coli* (3MZD)	PBP	-61.05	-55.10	1.645	ASN178,GLY55,MET58,LYS59
2.	1NZO	*E.coli* (1NZO)	PBP	-57.65	-51.92	1.645	ASN178,GLY55,LYS59,MET58
3.	3OC2	*Pseudomonas aeruginosa*	PBP	-66.5	-56.14	1.645	ASP172,ARG152,ASP169,VAL170, THR168,ASP171
4.	1TVF	*Staphylococcus aureus*	PBP	-57.01	-41.08	1.645	SER75,SER116,ASN141,LEU115
5.	Model 1	*Shigella dysenteriae*	PBP	-53.97	-53.97	1.645	GLN142,ARG166,VAL184
6.	Model 2	*Streptococcus pneumoniae*	PBP	-60.19	-41.93	1.645	ASN410,TRP411,ASP412,SER428
7.	Model 3	*Klebsiella pneumoniae*	PBP	-63.63	-54.48	1.645	ARG235,GLN270,TYR310
8.	Model 4	*Salmonella typhimurium*	PBP	-59.96	-51.49	1.645	THR413, GLN460, PRO412, GLY414, ALA499

The PBPs of *Escherichia coli* 3MZD and 1NZO (Fig. 5 and 6) both seem to have affinity for the amino acids ASN at 178th position, GLY at 55th position (Both predicted active sites) and LYS at 59th position forming 4

hydrogen bonds each. These results are in correlation with the wet lab results for *E.coli*. The PBP of *Pseudomonas aeurignosa* (Fig. 7) forms 6 hydrogen bonds of which ASP is the most targeted (3 Bonds) with interactions at 170,171 and 172th positions. This is evident by the highest docking score this interaction has compared to the others.

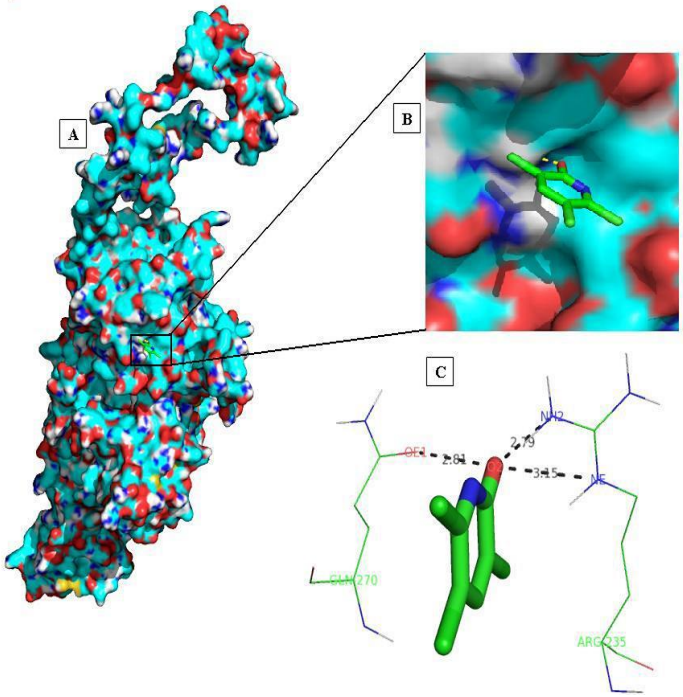

Figure 5: Docking results of *E.coli* (3MZD). (A). Binding mode of TCP with PBP of *E.coli.* (B). A close-up view of the binding site of TCP in PBP (3MZD). (C) TCP interaction with PBP. Ligand atoms are coloured by its type. Protein showed in surface model. The interacted amino acids residues, hydrogen bond networks in the binding pocket and the distance (in Angstrom units) of bonds are all shown.

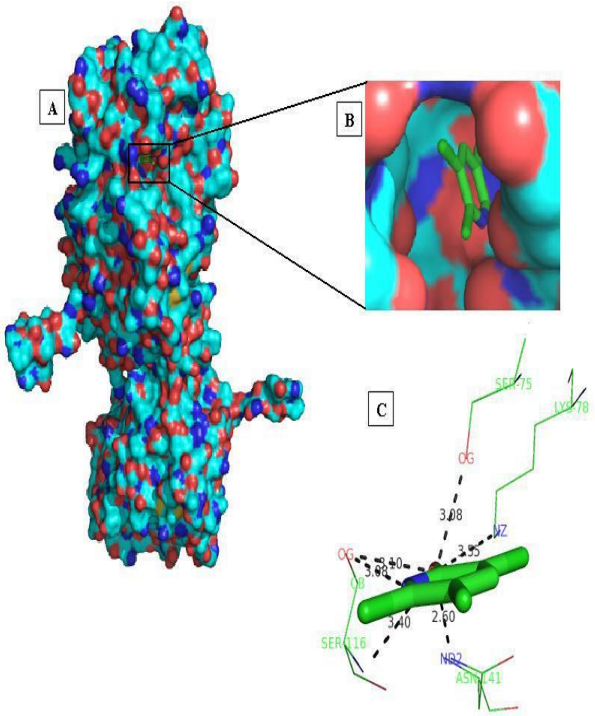

Figure 6: Docking results of *E.coli* (1NZO). (A). Binding mode of TCP with PBP of *E.coli.* (B). A close-up view of the binding site of TCP in PBP (1NZO). (C) TCP interaction with PBP. Ligand atoms are coloured by its type. Protein showed in surface model. The interacted amino acids residues, hydrogen bond networks in the binding pocket and the distance (in Angstrom units) of bonds are all shown.

ISSN: 0975-8585

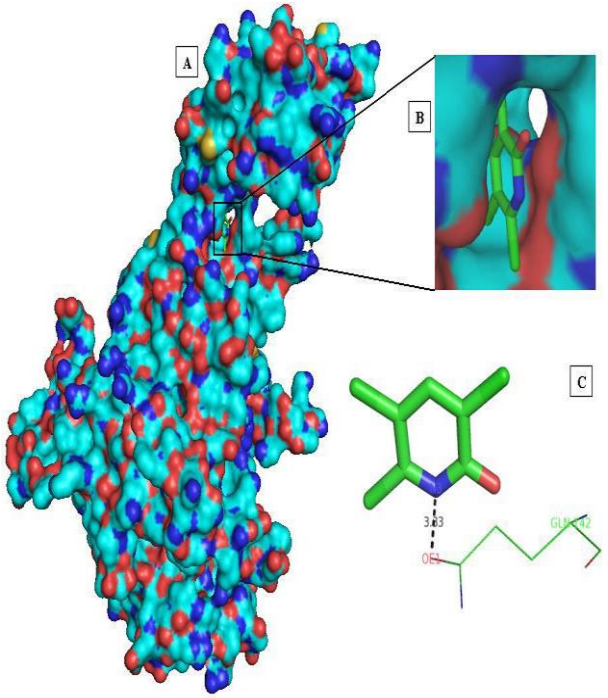

Figure 7: Docking results of *Pseudomonas aeurignosa* (3OC2). (A). Binding mode of TCP with PBP of *Pseudomonas aeurignosa.* (B). A close-up view of the binding site of TCP in PBP (3OC2). (C) TCP interaction with PBP. Ligand atoms are coloured by its type. Protein showed in surface model. The interacted amino acids residues, hydrogen bond networks in the binding pocket and the distance (in Angstrom units) of bonds are all shown.

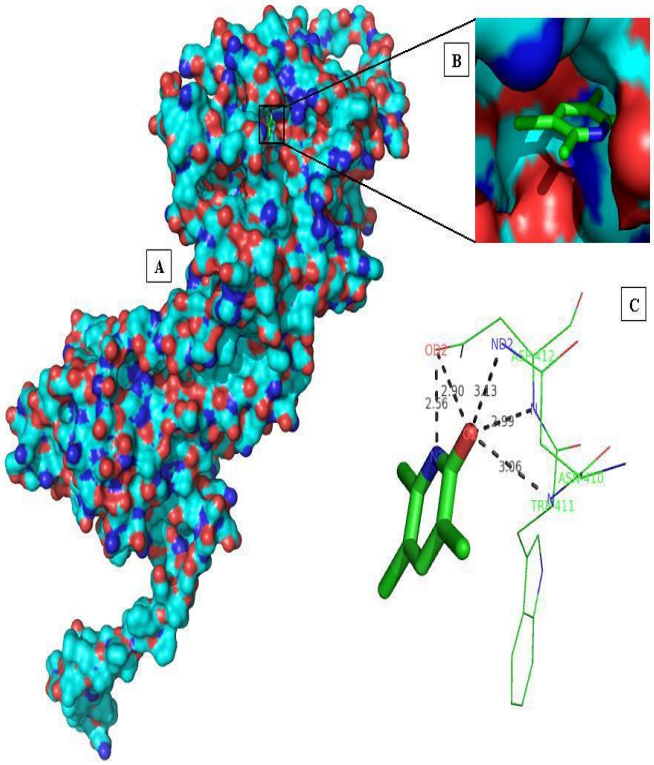

Figure 8: Docking results of *Streptococcus pneumoniae* (A). Binding mode of TCP with PBP of *Streptococcus pneumoniae* (B). A close-up view of the binding site of TCP with PBP. (C) TCP interaction with PBP. Ligand atoms are coloured by its type. Protein showed in surface model. The interacted amino acids residues, hydrogen bond networks in the binding pocket and the distance (in Angstrom units) of bonds are all shown.

ISSN: 0975-8585

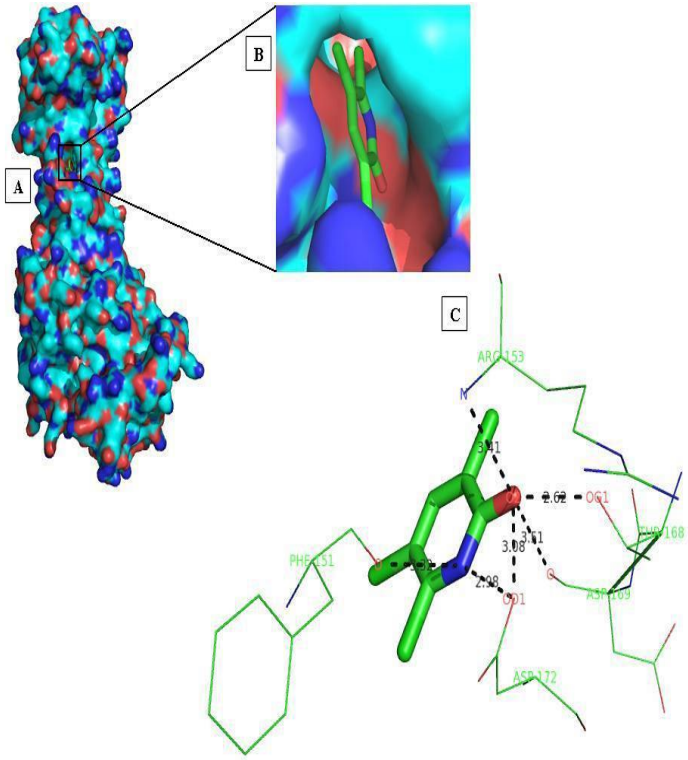

Figure 9: Docking results of *Shigella dysenteriae* (A). Binding mode of TCP with PBP of *Shigella dysenteriae* (B). A close-up view of the binding site of TCP with PBP. (C) TCP interaction with PBP. Ligand atoms are coloured by its type. Protein showed in surface model. The interacted amino acids residues, hydrogen bond networks in the binding pocket and the distance (in Angstrom units) of bonds are all shown.

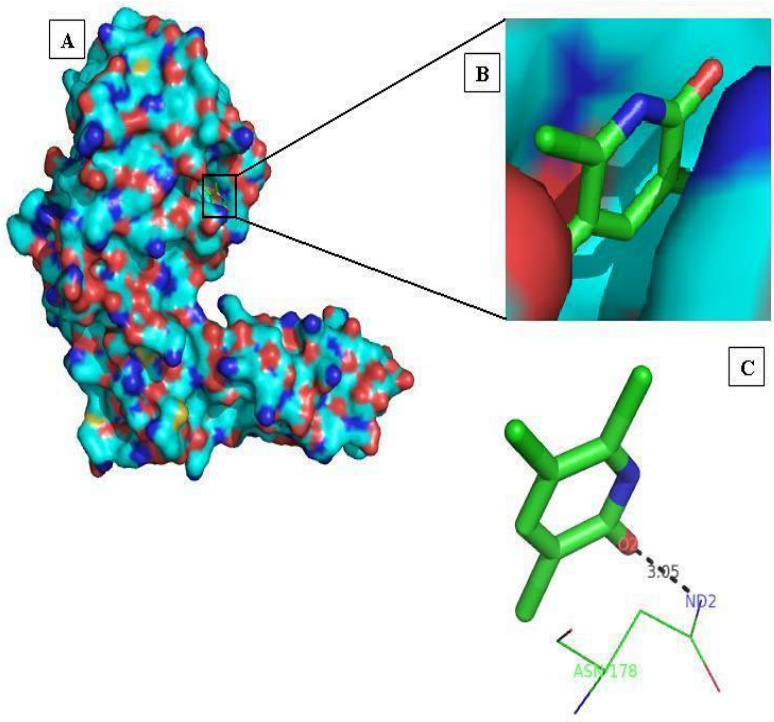

Figure 10: Docking results of *Staphylococcus aureus* (A). Binding mode of TCP with PBP of *Staphylococcus aureus*. (B). A close-up view of the binding site of TCP with PBP. (C) TCP interaction with PBP. Ligand atoms are coloured by its type. Protein showed in surface model. The interacted amino acids residues, hydrogen bond networks in the binding pocket and the distance (in Angstrom units) of bonds are all shown.

ISSN: 0975-8585

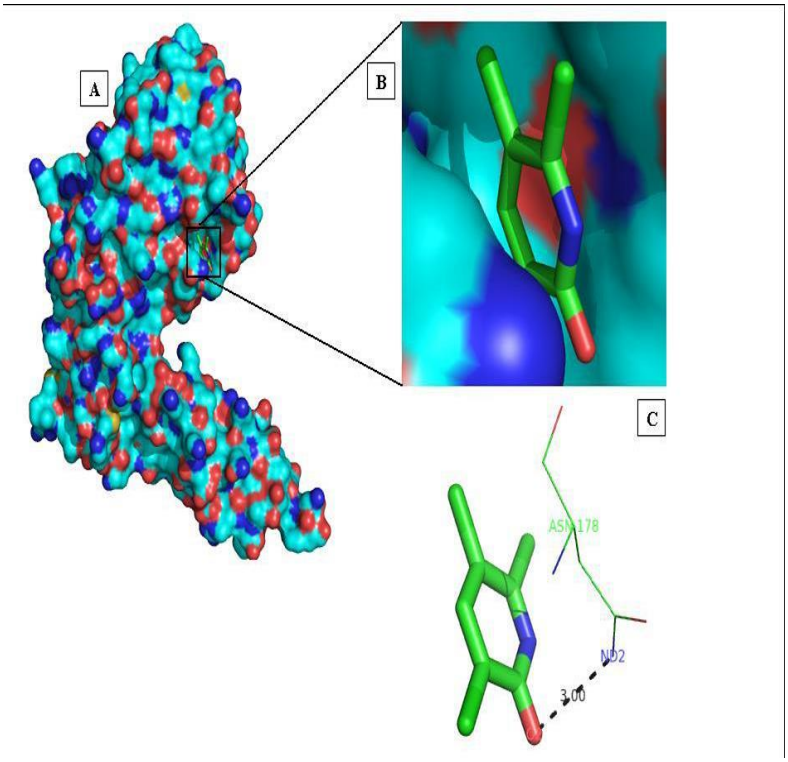

Figure 11: Docking results of *Klebsiella pneumoniae* (A).Binding mode of TCP with PBP of *Klebsiella pneumoniae* (B).A close-up view of the binding site of TCP with PBP. (C) TCP interaction with PBP. Ligand atoms are coloured by its type. Protein showed in surface model. The interacted amino acids residues, hydrogen bond networks in the binding pocket and the distance (in Angstrom units) of bonds are all shown.

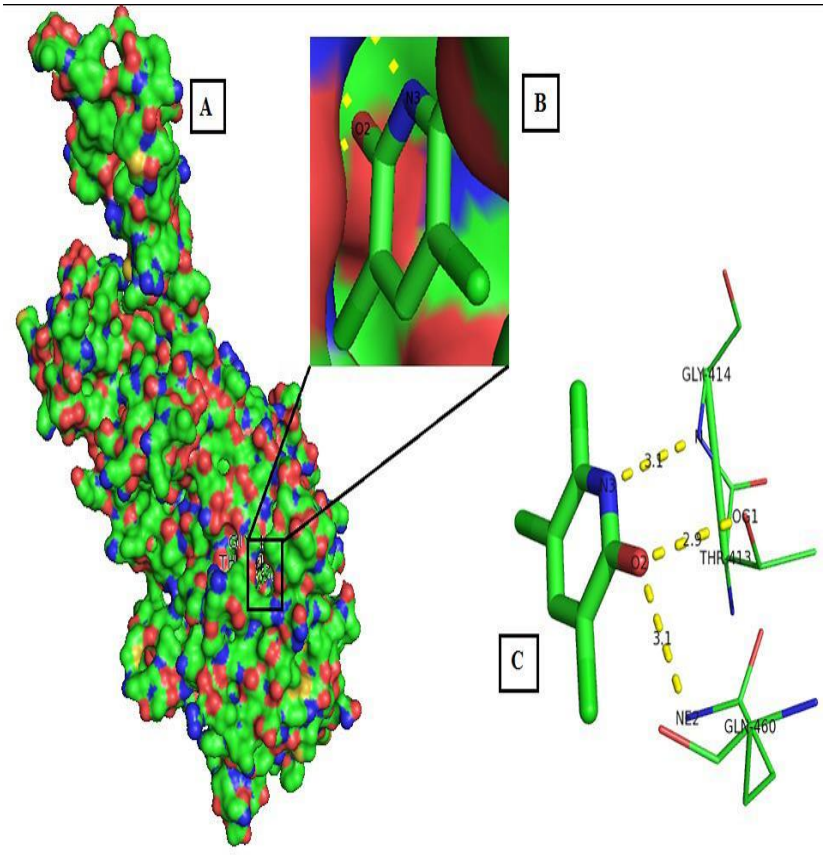

ISSN: 0975-8585

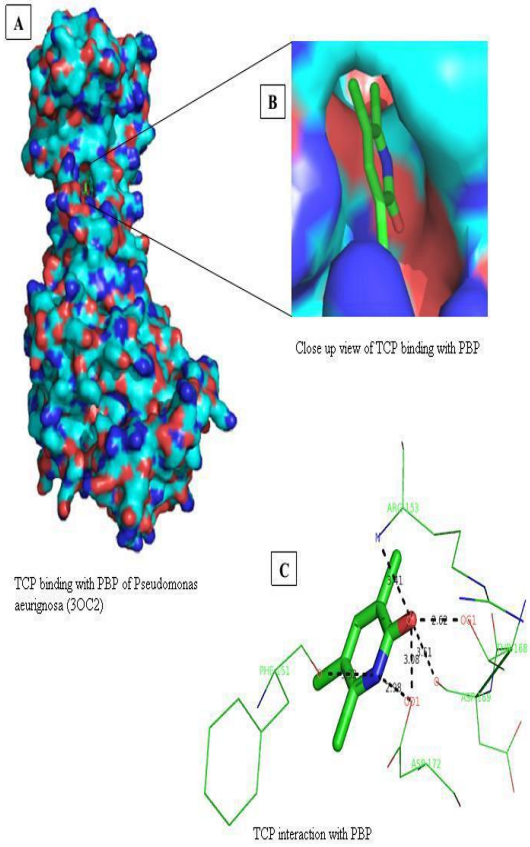

Figure 12: Docking results of *Salmonella typhimurium* (A).Binding mode of TCP with PBP of *Salmonella typhimurium* (B).A close-up view of the binding site of TCP with PBP. (C) TCP interaction with PBP. Ligand atoms are coloured by its type. Protein showed in surface model. The interacted amino acids residues, hydrogen bond networks in the binding pocket and the distance (in Angstrom units) of bonds are all shown.

PBP of *Streptococcus pneumoniae* has registered the third highest docking score of -60.19 with the help of strong hydrogen bond interactions with ASN at 410th position and TRP at 411th position. As predicted it has established interactions with active site residues ASP and SER in positions 412 and 428 respectively (Fig. 8).

The PBP of *Shigella dysenteriae* and *Staphylococcus aureus* have established interactions with the ligand molecule TCP. Interactions of TCP with *Shigella dysenteriae* (Fig. 9) resulted in hydrogen bond interactions with GLN, ARG, and VAL in positions 142, 166, 184 respectively. The ligand has established interactions with only three of the predicted active site residues with respect to *Staphylococcus aureus* (Fig.10) forming strong hydrogen bonds with the residues SER, ASN and LEU at positions 75, 116, 141 and 115 respectively resulting in lesser docking score.

The antimicrobial property of *Klebsiella pneumoniae,* outlined in Table 2 predicts that it is equally competent to *Pseudomonas aeurignosa*. In the same manner *Klebsiella pneumonia* (Fig. 11) has recorded the second highest docking score with the help of three strong hydrogen bonds with ARG at 235th position, GLN at 270th position (Both predicted active sites) and with TYR at 310th position.

CONCLUSIONS

From wetlab studies and docking results it is evident that TCP has a very good potential to be a likely drug candidate effective in the treatment of disorders arising out of *Pseudomonas aeruginosa*, *Klebsiella pneumonia*e, *E.coli* (3MZD) and *Streptococcus pneumoniae*. Results point out to it being effective in the treatment of Pneumonia.

ISSN: 0975-8585

REFERENCES

[1] Spellberg B, Powers JH, Brass EP, Miller LG, Edwards JE Jr. Clin Infect Dis 2004; 38: 1279–1286.
[2] McGowan JE. Rev Infect Dis 1983; 5:1033–48.
[3] Teresa M. Barbosa, Stuart B. Levy. Drug Resistant Updates 2000; 3: 303-311.
[4] Eric Batard, Florence Ollivier, David Boutoille, Jean-Beniot Hardouin, Emmanuel Montassier, Jocelyne Caillon, Francoise Ballereau. Int J Inf Dis 2013; 17: e254-e258.
[5] Adam C Palmer, Roy Kishony. Nat Rev Genet 2013; 14: 243–248.
[6] Thu Betteridge, John Merlino, Jonathon Natoli, Elaine YL Cheong, Thomas Gottlieb, H W Stokes. Microb Drug Resist 2013; 19 (2):104-109.
[7] Spellberg B, Guidos R, Gilbert, D. Bradley J, Boucher HW, Scheld WM, Bartlett JG, Edwards J Jr. Clin Infect Dis 2008; 46:155–164.
[8] Rossolini GM, Mantengoli E, Docquier JD, Musmanno RA, Coratza G. New Microbiol 2007; 30: 332–339.
[9] Meyer E, Schwab F, Schroeren-Boersch B, Gastmeier P. Crit Care 2010; 14: doi: 10.1186/cc9062.
[10] Rossi F, Baquero F, Hsueh PR, Paterson DL, Bochicchio GV, Snyder TA, Satishchandran V, McCarroll K, DiNubile M.J, Chow JW. J. Antimicrob Chemother 2006; 58:205–210.
[11] A.S.Csinos, Plant Disease 1985; 69:254-256.
[12] Chavan VP, Sonawane SA, Shingare MS, Karale BK. Chem Heterocyclic Comp 2006;42(5): 625-630.
[13] Sinosh Skariyachan, Rao Shruti Krishnan, Snehapriya Bangalore Siddapa, Chithra Salian. Bioinformation 2011;7(5): 222-233.
[14] MJ Alves, ICFR Ferreira, HJC Froufe, RMV Abreu, A Martins, M Pintado. J App Microbiol 2013; 1-12.
[15] Berman HM, Westbrook J, Feng Z, Gilliland G, Bhat TN, Weissig H, Shindyalov IN, Bourne PE. Nucleic Acids Res 2000; 28: 235-242.
[16] Pettersen EF, Goddard TD, Huang CC, Couch GS, Greenblatt DM, Meng EC, Ferrin TE. J Comput Chem; 2004; 25(13):1605-12.
[17] The UniProt Consortium. Nucleic Acids Res 2013; 41: D43-D47.
[18] Laskoswki RA, MacArthur MW, Moss DS, Thorton JM. J Appl Cryst 1993; 26: 283-291.
[19] Laurie AT, Jackson RM. Bioinformatics 2005; 21: 1908-1916.
[20] KC Hsu, YF Chen, SR Lin, JM Yang. BMC Bioinformatics 2011; 12 (Suppl1):S1-S33.
[21] Tarek A, El-Mihoub, Adrian A, Hopgood, Lars Nolle, Alan Battersby. Eng Lett 2006; 13:2. El_13_2_11.
[22] WatsonP, Verdonk M, Hartshorn MJA. J Mol Graphics Modelling 2003; 22:71-82.
[23] Christopher A. Lipinski, Franco Lombardo, Beryl W. Dominy, Paul J. Feeney. Adv. Drug Reviews 2001; 46:3-26.